ACS OMEGA

Open Access

http://pubs.acs.org/journal/acsodf

Article

Shear Performance in Reinforced Concrete Beams with Partial Aggregate Substitution Using Waste Glass: A Comparative Analysis via Digital Imaging Processing and a Theoretical Approach

Özer Zeybek, Boğaçhan Başaran, Ceyhun Aksoylu, Memduh Karalar, Essam Althaqafi, Alexey N. Beskopylny,* Sergey A. Stel'makh, Evgenii M. Shcherban', Osman Ahmed Umiye,* and Yasin Onuralp Özkılıç*

Cite This: *ACS Omega* 2024, 9, 41662−41675

Read Online

ACCESS | Metrics & More | Article Recommendations

ABSTRACT: The usage of waste glass aggregate (WGA) associated with the replacement of fine aggregate (FA) and coarse aggregate (CA) is observed to reduce the number of raw materials for sustainable concrete. For this aim, a total of 15 beams were produced, and then investigational experiments were implemented to observe the shear performances. The stirrup spacing and WGA proportion were chosen as the main parameters. FA and CA were exchanged with WGA with weight proportions of 0, 10, and 20%. The experimental investigation results showed that changing stirrup spacing and WGA proportion affected the fracture and shear properties of reinforced-concrete-beams (R-C-Bs). Furthermore, the findings of the test results revealed that the proportion of WGA could be efficiently consumed as 20% of the partial replacement of FA. With the addition of FA to the mixture, the load carrying capacity of R-C-Bs increases. On the other hand, increasing the WGA ratio by more than 10% using CA, together with increasing the stirrup spacing, can significantly reduce the capacity of R-C-Bs. It was observed that the calculated shear strengths of R-C-Bs with inadequate stirrup spacing, based on ACI 318 and EC2 design codes, can be up to 52 and 79% higher than the experimental results for R-C-Bs containing coarse glass aggregate and 21 and 56% higher for R-C-Bs containing fine glass aggregate, respectively. Additionally, an image processing method was applied to describe the damages/microdamages in R-C-Bs. At that point, the findings obtained from the experimental part of the study were confirmed by the results of the image processing method. Although the strains obtained with the image processing method are reliable, it has not been determined exactly where the crack will occur due to the very sudden development of the shear crack at the moment of beam failure.

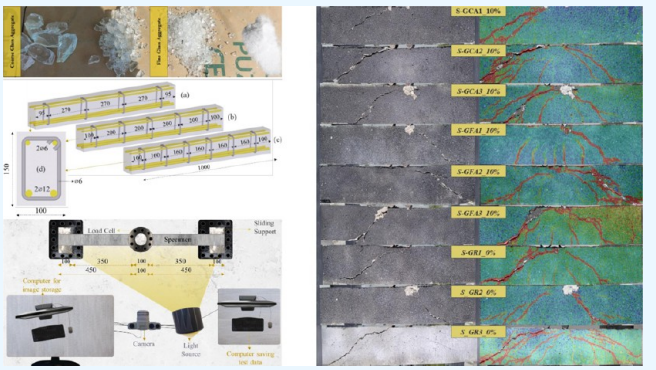

1. INTRODUCTION

One of the most often utilized building materials is concrete. This accelerates raw material consumption and pollutes the environment with CO_2 emissions. Different methods[1,2] prioritize green concrete manufacturing to address these concerns. These projects reduce CO_2 emissions and raw material use. Waste materials reduce raw material utilization. These waste products can be utilized for replacement of cement and aggregate. For example, waste materials such as tire, fire clay, marble, plastic, and others can be used instead of aggregate.[3−6] Glass is one of the waste materials that needs special handling and reprocessing techniques. There are several practices of consuming waste glass (WG) in the building industry over the world.[7−10] The chief challenge in using WG as an aggregate replacement is the alkali−silica rebound that occurs between the WG and the alkalis produced as a result of the cement during hydration.[11] This rebound can cause fractures in the concrete. For this reason, there is a need for a wide variety of research on the use of WG products in concrete and concrete products. One of these studies was implemented by Olofinnade et al.[12] In this investigation, Olofinnade et al.[12] investigated the impression of swapping both the natural FA and CA in the same combination with WG crushed to the same aggregate proportions on the strength development of concrete. At the end of this investigation, it was noticed that

Received: June 17, 2024
Revised: September 9, 2024
Accepted: September 12, 2024
Published: September 25, 2024

https://doi.org/10.1021/acsomega.4c05655
ACS Omega 2024, 9, 41662−41675

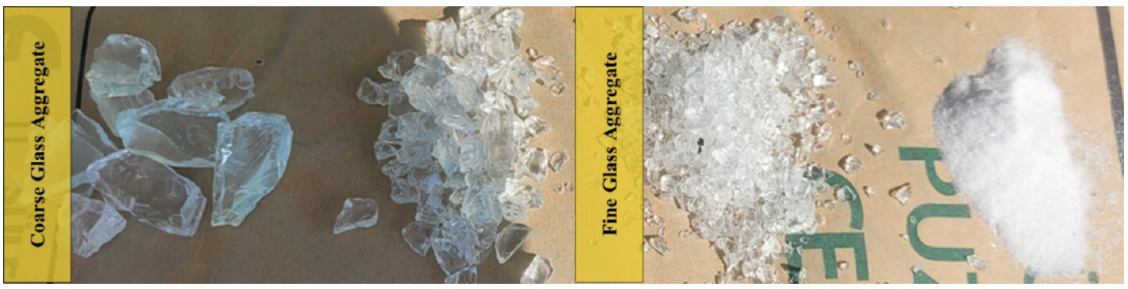

Figure 1. Glass coarse and fine aggregate samples.

Table 1. Results of Concrete with Fine and Coarse WG Aggregates[16]

no.	cube compressive strength (MPa)	cylinder compressive strength[a] (MPa)	increase rate (%)	splitting tensile strength (MPa)	increase rate (%)	flexural strength (MPa)	increase rate (%)
REF0%	18.89	15.11	0.0	1.33	0.0	6.26	0.0
FA10%	19.11	15.29	1.2	1.36	2.3	6.51	4.0
FA20%	20.89	16.77	10.6	1.39	4.5	6.67	6.5
CA10%	18.67	14.92	−1.2	1.29	−3.0	5.93	−5.3
CA20%	17.78	14.18	−5.9	1.24	−6.8	5.59	−10.7

[a]The equivalent cylinder CS was calculated using the interpolation between the cube and cylinder CS according to EN 206:2013 + A1:2016.[27]

there was a noteworthy decrease in the compressive strength and tensile strength. Tamanna et al.[13] used WG efficiently as a partial replacement for the sand in concrete. To do this, concrete was produced by replacing natural river sand with 20, 40, and 60% recycled glass sand. At the end of this investigation, the test implications presented a noteworthy enhancement in the strength of the concrete. Furthermore, it was also found that concrete made from WG also presented streamlined resistance to chloride ion penetration. Moreover, WG accumulation expressively reduced the extent of expansion caused by alkali-silica rebound. Rahim et al.[14] also investigated the properties of concretes having WG powder as FA. For this aim, WG powder was chosen as a partial replacement for sand at 10, 20, and 50% of concrete combinations. The implications evidenced that the compressive strength (CS) of samples with 10% WG powder was greater than that of the concrete control sample at 28 days. Arivalagan and Sethuraman[15] studied the properties of concrete with WG powder as FA. For this aim, WG powder was chosen as a partial replacement for sand at 10, 20, and 30% of concrete combinations. From this experimental investigation, it was confirmed that an increase in strength has been detected with the exchange of WG powder by natural sand. The other investigational study was implemented by Çelik et al.[16] In this investigation, Çelik et al.[16] chose powder and crushed WG to exchange coarse and FAs. As stated by the mechanical test, the WG forms an improved pozzolanic impression and increases the strength, whereas the glass particles tend to reduce the strength when they are exchanged with aggregates. Hama et al.[17] studied the structural behavior of R-C-Bs incorporating WG powder. In their study, WG was used as a substitute in cement weights of 0 (reference), 10, and 15%. Furthermore, nine beams were produced in this investigation. The effects of the WG on deflection productivity, longitudinal steel reinforcement on rebar, and transverse reinforcement intervals were also studied. Their study revealed that R-C-Bs containing WG powder had a higher deflection strength than those without. Haido et al.[18] focused on recycling WG powder as a silica fume replacement in high-strength concrete. The productivity of using WG powder instead of silica fume in a high-strength concrete beam deflection capacity was examined in this study. The findings showed that high strength concrete beams containing WG powder had a better vertical load capacity and ductility than those with silica fume. The research also found that WG powder is a viable alternative to pozzolanic silica fume powder. Sharba[19] investigated the impressions of waste ceramic tile aggregate combined with WG on the productivity of cementation combinations. For this purpose, WG was designed to exchange FA in proportions of 15, 30, and 45%. Consequently, it was noticed that by increasing the percentage of WG, the value of the ultimate load was improved, and also the formation of cracks was postponed. Amin et.al.[20] used experimental and machine learning approaches to determine the FS of cementitious composites with WG. WG at 0, 2.5, 5, 7.5, 10, 12.5, and 15% was used to partially replace cement and FA. WG replaced FA in cementitious composites with a 15% replacement rate, increasing the deflection strength by 36%. WG was better than fine aggregate, and the glass was pozzolanic, which may explain the increased deflection strength. Kumar et al.[21] evaluated the combined impression of WG employed as an FA substitute in different concentrations and reinforced with waste tire steel fibers. Mustafa et al.[22] analyzed the deflection productivity of RC beams having WG as a replacement to cement and FAs. The impression of the longitudinal steel proportion is also involved in the tests. Specifically, R-C-Bs with 10% WG increased cracking and ultimate loads by 29.0 and 6.9%, while R-C-Bs with 20% WG hardly affected them.

As mentioned above, in terms of mechanical properties and environmental aspects, the recycled WG was a good option for the replacement of raw materials.[23−26] Commonly, it is noticeable from the previous investigation attempts that WG might have a huge potential to be reused as raw aggregates. There is a lack of investigational studies of the effects of waste glass on structural members such as beams. This examination focuses on the deflection productivity of R-C-Bs counting WG as a replacement to FA and CA based on the research shortcomings of the existing studies.

https://doi.org/10.1021/acsomega.4c05655
ACS Omega 2024, 9, 41662−41675

2. MATERIALS AND METHOD

To procedure the beams, CEM I 32.5 Portland cement was taken into consideration for the mixture. The water-to-cement ratio was chosen as 0.50. Fine and coarse aggregates were replaced with WG at 10 and 20% by weight, respectively. The different particle sizes of WG utilized in this investigation are shown in Figure 1. The proportion of CA and FA was kept equal. It was selected that the proportion of cement to aggregates was 20%. It was observed that as the amount of WG used increased, the workability of the produced concrete decreased. Coarse aggregate in the size range of 5−13 mm and FA in the size range of 0−4 mm were utilized. Fine glass trash consists of an equal quantity of glass measuring 1.7−4 mm and 100−200 μm, whereas coarse glass waste consists of an equal amount of glass measuring 9−12 and 5−8 mm.

Three repeat cycles were performed for each mixture to compute the mechanical properties including compressive, splitting tensile, and flexural strength. Table 1 presents the mechanical properties of the test samples. According to Table 1, as the fine glass aggregate ratio increased, the capacities also increased. On the other hand, as the proportion of coarse glass aggregates increased, capacities decreased. More details can be found in ref 16.

Experimental examinations were carried out on the R-C-Bs in the Civil Engineering Laboratory at Necmettin Erbakan University, where the samples were produced. The dimensions of the R-C-Bs were chosen as 100 × 150 × 1000 mm. To investigate the shear behavior of the test samples, three different stirrup spacings of 27, 20, and 16 cm were considered. In the study, the beam shear span (a)/effective depth (d) ratio of all RCBs was 2.69. Figure 2 shows the details of the reinforcements of the R-C-B bonds, whereas Figure 3 shows the test setup.

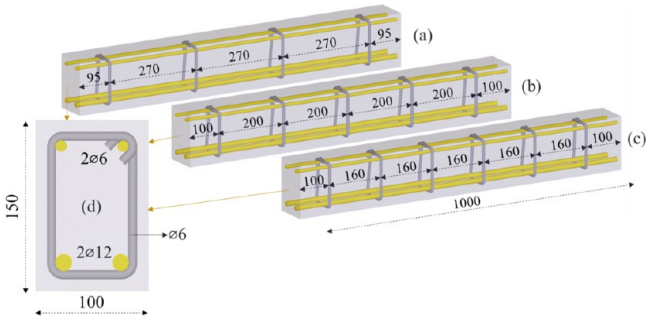

Figure 2. Reinforcement layout for samples with spacing of stirrup of (a) 270 mm, (b) 200 mm, and (c) 160 mm.

The replacement ratio of WG was the most important variable that was examined in this research; the stirrup spacing was a supplementary variable that was of interest. The characteristics of the individuals are detailed in Table 2.

3. EXPERIMENTAL TEST RESULTS AND DISCUSSION

3.1. Experimental Results. The test results of the beams subjected to the four-point bending test are summarized in Table 3. In Table 3, WGA is the replacement percentage of WG aggregate in concrete; δ_y, deflection (yield displacement) in the beams when the load level is $0.85P_{max}$; P_y, yield load ($0.85P_{max}$); S_y, yield stiffness (P_y/δ_y); δ_{Pmax}, the deflection of the beams when the load level is P_{max} (maximum deflection); P_{max}, maximum load; S_y, maximum stiffness (P_{max}/δ_{max}); δ_u, the deflection of the beams at the moment when the load level is $0.85P_{max}$, beyond P_{max} (final deflection); η, ductility (δ_u/δ_y); and δ_f, the deflection value at the end of the experiment. As can be seen from Tables 1 and 3, both the splitting tensile strength and bending strength of the concretes are related to each other and are also quite compatible with the shear strength results of the beams.

3.2. Effect of Stirrup Spacing Change on the Capacity of Beam Samples. *3.2.1. Situation 1: Load−Displacement Behavior of Reference R-C-Bs.* To determine the effect of the stirrup spacing on the cracks and capacity, the R-C-Bs with three different stirrup spacings were considered without any WGA. In this context, R-C-Bs with stirrup spacing of 270, 200, and 160 mm were tested in a four-point loading mechanism. The load−displacement curves obtained as a result of the test and the fracture patterns occurring in the beams are listed in Figure 4. As noted in Figure 4, for the spacing of stirrup designated as 270 mm, P_{max} was noticed as 41.70 kN, and the ultimate displacement (δ_u) was appointed as 5.17 mm. When the spacing of stirrup was designated as 200 mm, these values were increased to 48.16 kN and 7.42 mm. When the spacing of stirrup decreased to 160 mm, it was noticed that these values increased to 55.16 kN and 7.90 mm. When the crack patterns of the beams are analyzed, sudden shear failure occurred in S_GR1 and S_GR2 beams due to diagonal tension crack. However, in beam S_GR3, as a result of tightening the stirrup spacing more (160 mm), while the shear strength of the beam increased, the beam was forced to behave like a tied arch, although the failure was still a diagonal tension crack. Therefore, the crack started from the support and extended toward the loading point. In addition, the shear capacity of the beams increased as the stirrup spacing decreased. By decreasing the stirrup spacing from 270 to 200 mm, the shear capacity increased by 15.5%, and by decreasing the stirrup spacing from 200 to 160 mm, the shear capacity increased by 14.5%.

3.2.2. Situation 2: Load−Displacement Behavior of R-C-Bs with 10% GCA Replacement. In this part of the research, the effects of changes in stirrup spacing (270, 200, and 160 mm) on the shear behavior of the R-C-Bs with 10% glass coarse aggregate (GCA) replacement were examined. As seen in Figure 5, for the stirrup spacing selected as 270 mm, P_{max} was obtained as 39.58 kN, and the ultimate displacement (δ_u) was detected as 5.50 mm. When the spacing of the stirrup was chosen as 200 mm, these values were improved as 50.39 kN and 6.61 mm. Furthermore, it was observed that these values increased to 53.88 kN and 7.19 mm when the stirrup spacing was decreased to 160 mm. As associated with the above condition (situation 1), it might be noticed that as the percentage of the WGA streamlined from 0 to 10%, the vertical load−displacement capabilities of the R-C-Bs gradually increased as a result of the forthcoming existence of shear cracks in the R-C-Bs. As stirrup spacing decreases, R-C-Bs' vertical load−displacement capacities increase predictably. It was noticed that these values were parallel to situation 1. By decreasing the stirrup spacing from 270 to 200 mm, the shear capacity increased by 27.3%, and by decreasing the stirrup spacing from 200 to 160 mm, the shear capacity increased by 6.9%. When beams with 10% WGA additives are compared with reference beams, the shear strength of beams with 270 mm stirrup spacing decreased by 5.1%, whereas the shear strength of beams with 200 mm stirrup spacing increased by

https://doi.org/10.1021/acsomega.4c05655
ACS Omega 2024, 9, 41662−41675

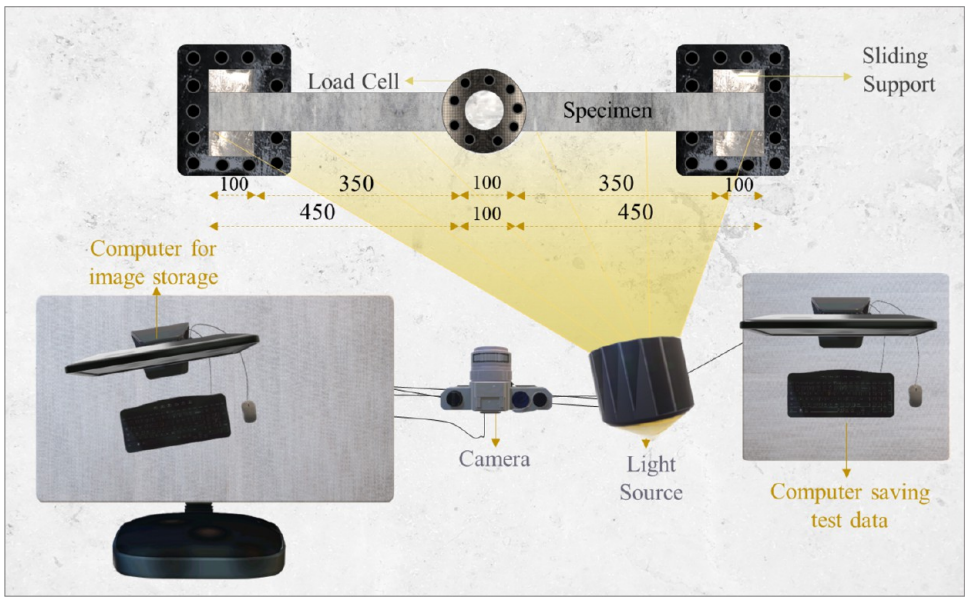

Figure 3. Test setup.

Table 2. Properties of Samples

no.	name	rep. aggregate	rep. (%)	stirrup spacing (mm)
1	S-GR1_0%		0	270
2	S-GR2_0%		0	200
3	S-GR3_0%		0	160
4	S-GCA1_10%	coarse	10	270
5	S-GCA2_10%	coarse	10	200
6	S-GCA3_10%	coarse	10	160
7	S-GCA4_20%	coarse	20	270
8	S-GCA5_20%	coarse	20	200
9	S-GCA6_20%	coarse	20	160
10	S-GFA1_10%	fine	10	270
11	S-GFA2_10%	fine	10	200
12	S-GFA3_10%	fine	10	160
13	S-GFA4_20%	fine	20	270
14	S-GFA5_20%	fine	20	200
15	S-GFA6_20%	fine	20	160

4.6% and the shear strength of beams with 160 mm stirrup spacing increased by 2.3%.

3.2.3. Situation 3: Load−Displacement Behavior of R-C-Bs with 20% GCA Replacement. In this section, stirrup spacing (270, 200, and 160 mm) in beams with 20% coarse glass aggregate replacement was examined for shear capacity and fracture forms. As seen in Figure 6, for the stirrup spacing determined as 270 mm, P_{max} was determined as 36.09 kN and δ_u was obtained as 6.05 mm. When the stirrup spacing was taken as 200 mm, these values were found to be 44.05 kN and 5.10 mm. Additionally, when the spacing of the stirrup was reduced to 160 mm, these values were 45.01 kN and 9.40 mm. As associated with the above situations (situations 1 and 2), it may be observed that as the percentage of the WGA changed to 20%, the vertical load−displacement capabilities of the R-C-Bs gradually reduced. Moreover, the effect of stirrup location on the vertical load−displacement capabilities of R-C-Bs is noticed; as expected, as the spacing of stirrup reduces, the vertical load−displacement capabilities of the R-C-Bs gradually increase. It was observed that these values were comparable to those of situations 1 and 2. At the same time, the fracture patterns of the beams showed a similar behavior. As a result of

Table 3. Test Results Obtained from the Four-Point Bending Test

test no.	WGA (%)	δ_y (mm)	P_y (kN)	S_y (kN/mm)	δ_{Pmax} (mm)	P_{max} (kN)	S_{Pmax} (kN/mm)	$\delta_u(mm)$	η	δ_f (mm)	failure type
S-GR1	0	2.87	35.44	12.35	3.52	41.70	11.86	5.17	1.80	6.92	shear
S-GR2	0	3.75	40.94	10.92	6.73	48.16	7.16	7.42	1.98	8.89	shear
S-GR3	0	5.20	46.88	9.02	6.62	55.16	8.33	7.90	1.52	10.22	shear
S-GCA1	10	3.08	33.64	10.93	4.76	39.58	8.32	5.50	1.79	8.18	shear
S-GCA2	10	3.87	42.83	11.05	6.19	50.39	8.14	6.61	1.71	8.77	shear
S-GCA3	10	4.00	45.80	11.44	5.02	53.88	10.73	7.19	1.80	13.41	shear
S-GCA4	20	3.95	30.68	7.77	5.49	36.09	6.58	6.05	1.53	8.79	shear
S-GCA5	20	3.51	37.44	10.68	4.52	44.05	9.76	5.10	1.45	10.23	shear
S-GCA6	20	5.62	38.26	6.81	7.74	45.01	5.81	9.40	1.68	11.47	shear
S-GFA1	10	3.11	37.42	12.02	3.77	44.02	11.68	4.37	1.40	5.83	shear
S-GFA2	10	4.46	45.17	10.13	6.18	53.14	8.60	6.24	1.40	9.93	shear
S-GFA3	10	4.16	49.59	11.91	7.00	58.34	8.33	7.71	1.85	13.94	shear
S-GFA4	20	3.26	39.29	12.05	4.41	46.23	10.49	4.67	1.43	7.31	shear
S-GFA5	20	4.40	46.28	10.51	5.92	54.44	9.19	5.96	1.35	10.43	shear
S-GFA6	20	4.27	49.04	11.48	9.05	57.69	6.38	12.37	2.90	15.68	shear

https://doi.org/10.1021/acsomega.4c05655
ACS Omega 2024, 9, 41662−41675

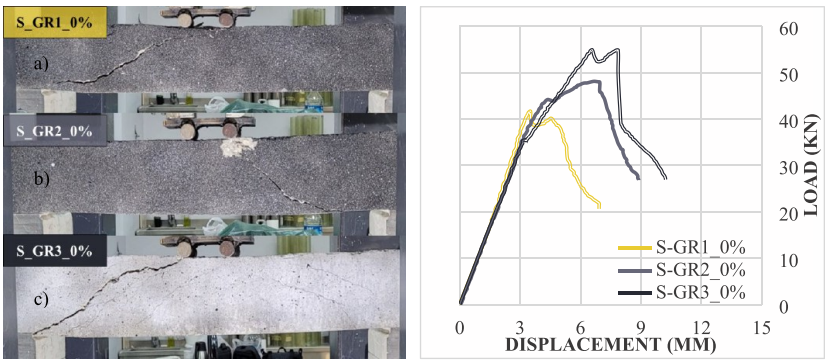

Figure 4. Assessment of failure patterns for 0% GCA with spacing of stirrup of (a) 270 mm, (b) 200 mm, and (c) 160 mm.

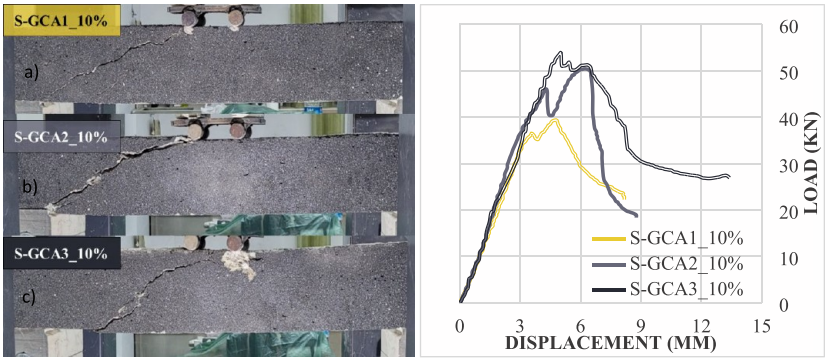

Figure 5. Assessment of failure patterns for 10% GCA with spacing of stirrup of (a) 270 mm, (b) 200 mm, and (c) 160 mm.

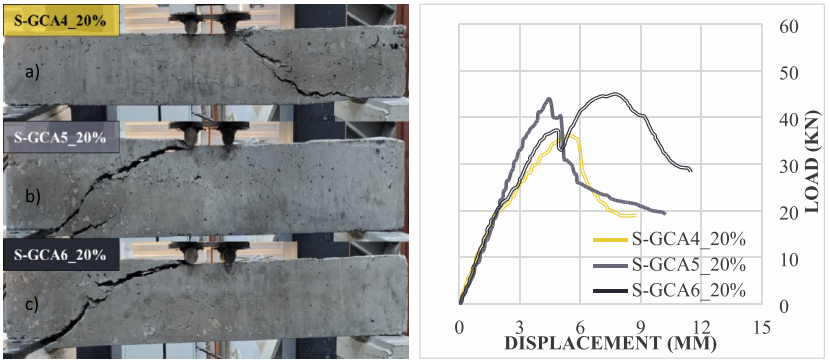

Figure 6. Assessment of failure patterns for 20% GCA with spacing of stirrup of (a) 270 mm, (b) 200 mm, and (c) 160 mm.

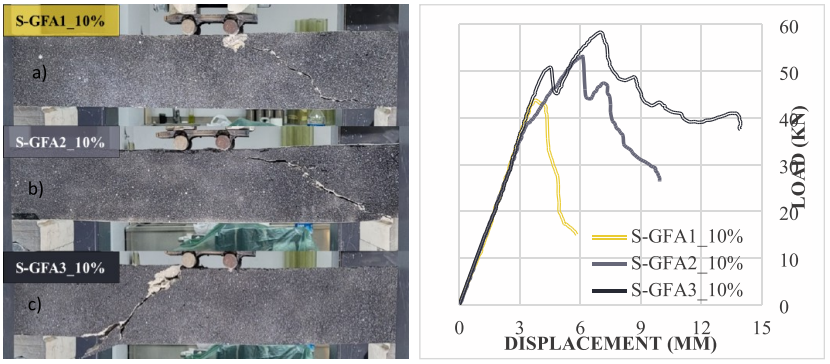

Figure 7. Assessment of failure patterns for 10% GFA with spacing of stirrup of (a) 270 mm, (b) 200 mm, and (c) 160 mm.

reducing the stirrup spacing from 270 to 200 mm in beams that included 20% WGA additives, the shear capacity of the beam improved by 22.1%. Additionally, the shear capacity increased by 2.2% when the stirrup spacing was reduced from 200 to 160 mm. When beams with 20% GCA additives were compared with reference beams, the shear strengths of beams

https://doi.org/10.1021/acsomega.4c05655
ACS Omega 2024, 9, 41662−41675

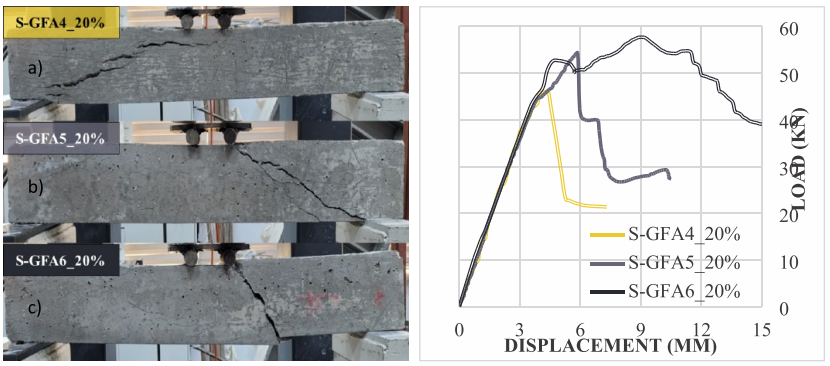

Figure 8. Assessment of failure patterns for 20% GFA with spacing of stirrup of (a) 270 mm, (b) 200 mm, and (c) 160 mm.

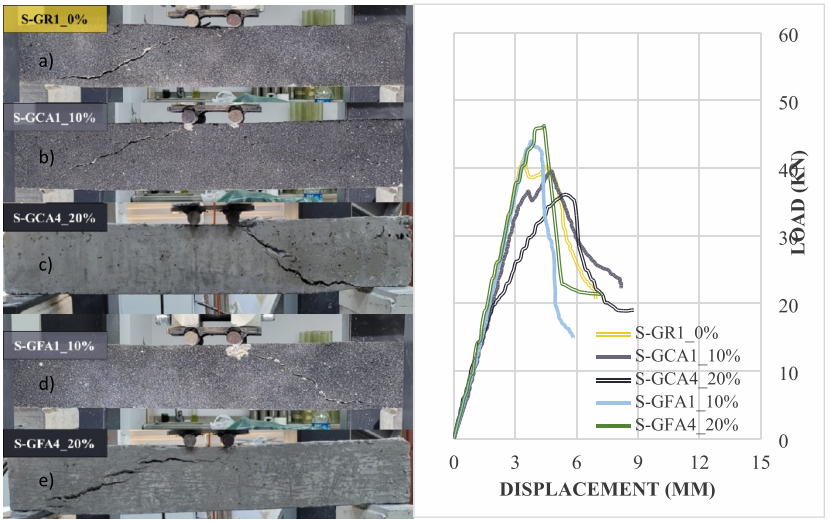

Figure 9. Assessment of failure patterns of R-C-Bs with 270 mm stirrup spacing: (a) S-GR1_0%, (b) S-GCA1_10%, (c) S-GCA4_20%, (d) S-GFA1_10%, and (e) S-GFA4_20%.

with 270, 200, and 160 mm stirrup spacing decreased by 13.4, 8.5, and 18.4%, respectively.

3.2.4. Situation 4: Load–Displacement Behavior of R-C-Bs with 10% GFA Replacement. In this section, the effects of changes in stirrup spacing on the shear behavior of R-C-Bs with a 10% glass fine aggregate (GFA) replacement were investigated. In this context, beams with 270, 200, and 160 mm stirrup spacings were examined, similar to cases 1, 2, and 3, and their shear properties were compared with both reference beams and also GCA substituted beams. As noted in Figure 7, for the spacing of stirrup chosen as 270 mm, P_{max} was found as 44.02 kN and δ_u as 4.37 mm. When the spacing of the stirrup was chosen as 200 mm, these values were improved as 53.14 kN and 6.24 mm. Moreover, when the spacing of the stirrup decreased to 160 mm, it was noticed that these values improved to 58.34 kN and 7.71 mm. As expected, all of the beams collapsed as a result of diagonal shear cracks due to insufficient stirrup spacing. When stirrup spacings were reduced from 270 to 200 mm and 200 to 160 mm, beam shear capabilities increased by 20.7 and 9.8%, respectively. Compared to the reference beams, shear capacities increased by 5.6% for 270 mm stirrup spacing, 10.3% for 200 mm, and 5.8% for 160 mm. Similarly, the shear strengths of beams with 10% GFA replacement were found to be 11.2, 5.5, and 8.3% higher, respectively, than those of beams with 10% GCA replacement.

3.2.5. Situation 5: Load–Displacement Behavior of R-C-Bs with 20% GFA Replacement. In this part of the investigation, 20% WGA was replaced with FA to examine the effect of GFA with a stirrup arrangement on shear performance. When the fracture patterns of the beams are examined (Figure 8), it can be seen that they are the same as the fourth case and that they collapsed through the diagonal shear crack. However, due to the small stirrup spacing in the third row beams (160 mm), it can be seen that the shear crack was forced to propagate through the concrete between the stirrups. Considering that the diagonal shear crack occurred between the support and the loading point in the reference beam, there were small differences in the behavior of the shear fracture. These discrepancies, on the other hand, are deemed to be typical when one considers the complicated behavior of shear fracture. When the stirrup spacings were reduced from 270 to 200 mm, the shear capacities of the beams increased by 17.8%, and when they were reduced from 200 to 160 mm, the shear capacities of the beams increased by 6.0%. Compared to the reference beams, shear capacities increased by 10.9, 13.0, and 4.6% for stirrup spacings of 270, 200, and 160 mm, respectively. Similarly, the shear strengths of beams with 20% GFA replacement were found to be 28.1, 23.6, and 28.2% higher, respectively, than those of beams with 20% GCA replacement. When the flexural strengths of GFA substituted concretes are examined, their bending strengths increased by

https://doi.org/10.1021/acsomega.4c05655
ACS Omega 2024, 9, 41662−41675

Table 4. Change Rates of Concrete Compressive and Bending Strengths, Maximum Strengths of Beams, and Yield Stiffnesses Relative to Each Other (%)

changing	CS	FS	$P_{max,270}$	$S_{y,270}$	$P_{max,200}$	$S_{y,200}$	$P_{max,160}$	$S_{y,160}$
CA10/CA20	5.0	6.1	9.7	40.7	14.4	3.46	19.7	68.0
REF/CA10	1.2	5.6	5.4	13.0	−4.4	−1.17	2.4	−21.2
FA10/REF	1.2	4.0	5.6	−2.7	10.3	−7.2	5.8	32.0
FA20/FA10	9.3	2.5	5.0	0.2	2.4	3.8	−1.1	−3.6

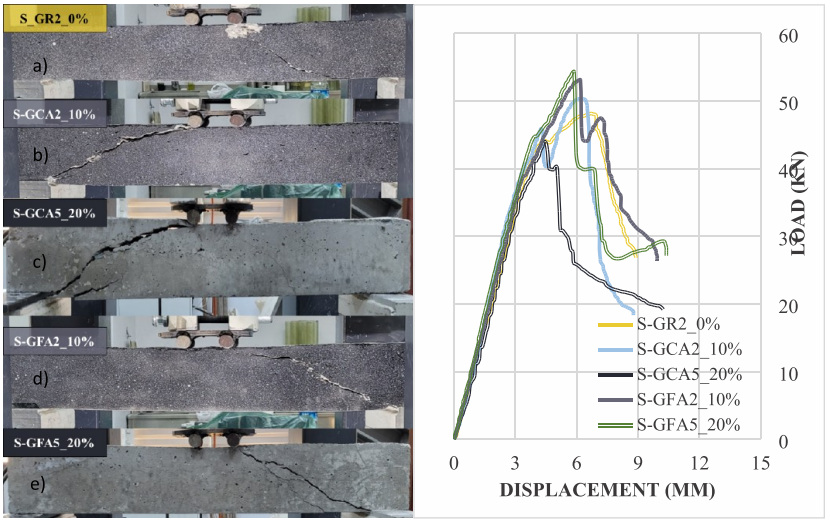

Figure 10. Assessment of failure patterns of R-C-Bs with 200 mm stirrup spacing: (a) S-GR2_0%, (b) S-GCA2_10%, (c) S-GCA5_20%, (d) S-GFA2_10%, and (e) S-GFA5_20%.

6.5 and 19.3% compared to those of the reference and GCA substituted concretes, respectively.

As can be seen in Figures 4−8, as expected, as the stirrup spacing decreased in all samples, whether with or without glass aggregate, the shear force carrying capacity of the beams increased ($P_{max,270\ mm} < P_{max,200\ mm} < P_{max,160\ mm}$). As expected, this occurred because the shear stress rate carried by the stirrups increased as the stirrup spacing decreased.

3.3. Effect of WGA Amount on Load−Displacement Behavior. This section examines how 10 and 20% glass aggregate replacement rates affect the beam shear capacity and fracture pattern in beams with the same stirrup spacing. At the same time, the effects of the waste glass substitution type (fine glass aggregate and coarse glass aggregate) on the beam shear properties were compared with each other in beams with the same stirrup spacing and waste glass replacement percentage.

3.3.1. Situation 6: Load−Displacement Behavior of R-C-Bs with 270 mm Stirrup Spacing. The shear behaviors of beams with a stirrup spacing of 270 mm are compared with one another in this subsection. The comparison is made according to the form of the WG (GFA and GCA) and the replacement rates of WGA from concrete. As can be seen from Figure 9, the maximum shear strength of the beams increased from a high rate of coarse glass aggregate substitution to a high rate of fine glass aggregate substitution ($P_{max,S\text{-}GCA4\_20\%} < P_{max,S\text{-}GCA1\_10\%} < P_{max,S\text{-}GR1\_0\%} < P_{max,S\text{-}GFA1\_10\%} < P_{max,S\text{-}GFA4\_20\%}$). As seen from Table 3, this situation is parallel to the mechanical strengths of concrete. As a result of the very high stirrup spacing in these beams, the shear loads that are produced by the beams are mostly supported by plain concrete. The situation becomes much clearer when the changes between the compressive and bending strengths, beam shear capacities, and yield stiffness of these concretes are compared to each other (Table 4). As can be seen from Table 4, rather than the change in the concrete compressive strength, the changes in the bending strength of the concrete and the shear strength of the beams are quite close to each other.

The yield stiffness of the beams was parallel to the maximum shear strength of the beam. As the rate of GCA in concrete increased (10 and 20%), the yield stiffness of the beams decreased by 11.5 and 37.1%, respectively, compared with the reference beam. The rate of GFA reduced the yield stiffness by approximately 2.5% in both substitutions compared to that of the reference beam.

3.3.2. Situation 7: Load−Displacement Behavior of R-C-Bs with 200 mm Stirrup Spacing. In this subsection, the shear behaviors of beams with 200 mm stirrup spacing are compared with each other according to the shape of the WG (GFA and GCA) and the substitution rates of WGA in concrete. As can be seen from Figure 10, the maximum shear strength of the beams increased from a high rate of GCA substitution rate to a high rate of GFA substitution (except for the S-GCA2_10% beam) ($P_{max,S\text{-}GCA5\_20\%} < P_{max,S\text{-}GR2\_0\%} < P_{max,S\text{-}GFA2\_10\%} < P_{max,S\text{-}GFA5\_20\%}$). However, because the stirrup spacing in beams with 200 mm stirrup spacing is reduced compared to the beams in condition 6 (270 mm), the beam shear behavior has begun to be controlled with stirrups instead of plain concrete. As can be seen from Table 4, an irregularity began between the increases in concrete compressive and bending strengths and the shear strengths of the beams (the increases were regular in the beams with 270 mm stirrup spacing). This situation is thought to be due to the shear stress sharing between the concrete and the stirrup, affecting the initial conditions of the sudden and brittle shear crack. However, although the shear strength increase rates are regular, GCA substitution (20%) reduced the shear strength of the beam by

https://doi.org/10.1021/acsomega.4c05655
ACS Omega 2024, 9, 41662−41675

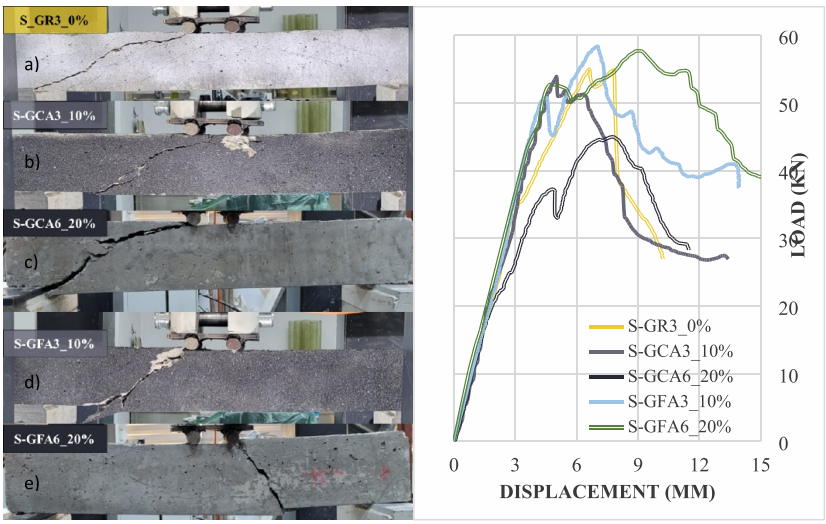

Figure 11. Assessment of failure patterns of R-C-Bs with 160 mm stirrup spacing of (a) S-GR3_0%, (b) S-GCA3_10%, (c) S-GCA6_20%, (d) S-GFA3_10%, and (e) S-GFA6_20%.

up to 9% compared to the reference beam, and GFA substitution (20%) increased it by up to 13%.

3.3.3. Situation 8: Load−Displacement Behavior of R-C-Bs with 160 mm Stirrup Spacing. In this subsection, the shear behaviors of beams with 160 mm stirrup spacing are compared with each other according to the shape of the WG (GFA and GCA) and the substitution rates of the glass aggregate in concrete (Figure 11 and Table 4). In Figure 11, the load−displacement curves of the beams are presented. As can be seen from the figure, with increasing spacing of stirrups, the shear capacities of the beams have become very close to each other (except for 20% GCA). As the stirrup spacing decreased, the maximum shear strengths of GCA (10%) and GFA (10 and 20%) substituted beams were almost similar to those of the reference beam. There was a minimal change in the initial stiffness of the beams. The most significant explanation for these kinds of situations can be shown to be the fact that the stirrups cover a large part of the shear stresses that are present in the beam. This is because the stirrups are very close together. However, as can be seen from the load−displacement curves of the beams, as the loading level approached the maximum force in the tests, the curves in the beams started to yield at different points. This situation changed depending on the initial conditions of the shear cracks in the beams. For this reason, it was thought that it would not be correct to compare the yield stiffness of beams, as the comparison of yield stiffness would be inaccurate.

As can be seen in Figures 9−11, substitution of 10 and 20% coarse glass aggregate in the beams can reduce the shear capacity of the beams by up to 5 and 18%, respectively, compared to the reference beam, depending on the stirrup spacing. However, substitution of 10 and 20% fine glass aggregates in the beams can increase the shear capacity of the beams by at least 4.6% compared to the reference beam. Although the initial stiffness of WGA-added beams is almost similar to the initial stiffness of the reference beam, stiffness deterioration in coarse glass aggregate-added beams appears at lower load levels. However, beams containing fine glass aggregate can almost maintain their rigidity up to a maximum load compared to the reference beam. It was observed that the substitution of coarse glass aggregate had a negative effect on the shear behavior of the beams and that the substitution of fine glass aggregate had a positive effect. For these reasons, it can be said that waste glass aggregates can be used carefully in beams, up to 10% instead of coarse aggregate in coarse form and up to 20% in fine form.

4. COMPARISON OF EXPERIMENTAL SHEAR STRENGTHS WITH VALUES RECOMMENDED BY INTERNATIONAL STANDARDS

In the study, the methods recommended in EC2[28] and ACI 318-19[29] were used to calculate the shear capacities of beams. Safety factors were not used in the shear capacity calculations of the beams. While calculating the shear capacity of the beam (V_n) in EC2,[28] the contribution of the concrete (V_c, eq 1) and the contribution of the stirrup (V_s, eq 5) were calculated separately, and the larger one was considered as the shear capacity of the beam. In EC2,[28] a method based on the plastic truss analogy was used to calculate the shear force carried by the stirrup. In this method, the angle (θ) of the compression struts with the beam axis is variable. Equations 1−6 were used in the shear calculation of experimental beams according to EC2.[28]

$$V_c = 0.18k(100\rho f_c)^{1/3} b_w d \le V_{max} \quad (1)$$

$$k = 1 + \sqrt{\frac{200}{d}} \le 2 \quad (2)$$

$$V_{c,min} = 0.035k^{3/2}\sqrt{f_c}\, b_w d \quad (3)$$

$$\nu_1 = 0.6\left[1 - \frac{f_c}{250}\right] \quad (4)$$

$$V_s = \frac{A_{sw}}{s} 0.9 d f_{ywk} \cot\theta \le V_{max} \quad (5)$$

$$V_{max} = \frac{\alpha_{cw} b_w 0.9 d \nu_1 f_c}{\cot\theta + \tan\theta} \quad (6)$$

where k is the size effect modification factor, f_c is the cylinder CS (MPa), ρ is the tensile reinforcement ratio ($\rho = A_s/b_w d \le 0.02$), A_s is the longitudinal tensile reinforcement area (mm^2), b_w is the width of the beam (mm), d is the effective depth

https://doi.org/10.1021/acsomega.4c05655
ACS Omega 2024, 9, 41662−41675

Table 5. Calculated Shear Values according to EC2[28] and Comparison with Experimental Results

test no.	rep.[a] (%)	stirrup spacing (mm)	$V_{exp.}$ (kN)	$V_{c,min}$ (kN)	V_{max} (kN)	V_c (kN)	V_s (kN)	V_n (kN)	V_n/V_{exp}
S-GR1	0	270	20.85	5.00	34.36	13.91	34.31	34.31	1.65
S-GR2	0	200	24.08	5.00	34.36	13.91	46.32	34.36	1.43
S-GR3	0	160	27.58	5.00	34.36	13.91	57.90	34.36	1.25
S-GCA1	10	270	19.79	4.97	33.97	13.86	34.31	33.97	1.72
S-GCA2	10	200	25.20	4.97	33.97	13.86	46.32	33.97	1.35
S-GCA3	10	160	26.94	4.97	33.97	13.86	57.90	33.97	1.26
S-GCA4	20	270	18.05	4.85	32.38	13.62	34.31	32.38	1.79
S-GCA5	20	200	22.03	4.85	32.38	13.62	46.32	32.38	1.47
S-GCA6	20	160	22.51	4.85	32.38	13.62	57.90	32.38	1.44
S-GFA1	10	270	22.01	5.03	34.75	13.97	34.31	34.31	1.56
S-GFA2	10	200	26.57	5.03	34.75	13.97	46.32	34.75	1.31
S-GFA3	10	160	29.17	5.03	34.75	13.97	57.90	34.75	1.19
S-GFA4	20	270	23.12	5.27	37.87	14.41	34.31	34.31	1.48
S-GFA5	20	200	27.22	5.27	37.87	14.41	46.32	37.87	1.39
S-GFA6	20	160	28.85	5.27	37.87	14.41	57.90	37.87	1.31

[a]rep.: replacement ratio.

Table 6. Calculated Shear Values according to ACI[29] and Comparison with Experimental Results

test no.	rep.[a] (%)	stirrup spacing (mm)	$V_{exp.}$ (kN)	V_c (kN)	$V_{c,max}$ (kN)	V_s (kN)	$V_{s,max}$ (kN)	V_n (kN)	V_n/V_{exp}
S-GR1	0	270	20.85	8.64	21.22	15.25	33.35	23.89	1.15
S-GR2	0	200	24.08	8.64	21.22	20.58	33.35	29.22	1.21
S-GR3	0	160	27.58	8.64	21.22	25.73	33.35	34.37	1.25
S-GCA1	10	270	19.79	8.59	21.09	15.25	33.14	23.84	1.20
S-GCA2	10	200	25.20	8.59	21.09	20.58	33.14	29.17	1.16
S-GCA3	10	160	26.94	8.59	21.09	25.73	33.14	34.32	1.27
S-GCA4	20	270	18.05	8.37	20.56	15.25	32.31	23.62	1.31
S-GCA5	20	200	22.03	8.37	20.56	20.58	32.31	28.96	1.31
S-GCA6	20	160	22.51	8.37	20.56	25.73	32.31	34.10	1.52
S-GFA1	10	270	22.01	8.69	21.35	15.25	33.55	23.94	1.09
S-GFA2	10	200	26.57	8.69	21.35	20.58	33.55	29.28	1.10
S-GFA3	10	160	29.17	8.69	21.35	25.73	33.55	34.42	1.18
S-GFA4	20	270	23.12	9.10	22.36	15.25	35.13	24.35	1.05
S-GFA5	20	200	27.22	9.10	22.36	20.58	35.13	29.69	1.09
S-GFA6	20	160	28.85	9.10	22.36	25.73	35.13	34.83	1.21

[a]rep.: replacement ratio.

(mm), α_{cw} is assumed to be 1.0 for nonprestressed concrete members, ν_1 is a modification factor of strength reduction for concrete cracked in shear, A_{sw} is the transverse reinforcement area (mm^2), s is the spacing of transverse reinforcement (mm), f_{ywk} is the yield strength of steel reinforcement (MPa), and θ is the angle of the compression strut (°).

According to the plastic truss analogy, the compression bars in the beams remain within the support region. For this reason, while calculating the angle of the compression strut with the beam axis, the angle of the line drawn from the end of the support to the loading point with the beam axis (θ = 18.4°) was calculated. However, EC2[28] limits this angle to a minimum of 21.8 and 45°. Therefore, the compression bar angle of 21.8° was used in the calculations. Considering EC2[28] proposals, shear capacity values were compared with experimental results. The results obtained are presented in Table 5.

In ACI 318-19,[29] the contribution of concrete to the shear capacity is not neglected in the calculation of the shear capacity of the beam (V_n, eq 9). Therefore, a calculation method is recommended in which concrete (V_c, eq 7) and stirrup (V_s, eq 8) both contribute to the shear capacity. In ACI,[29] a method based on the classical truss analogy is used to calculate the shear force carried by the stirrup. In this method, the angle between the compression struts and beam axis is considered constant (45°). Equations 7−9 were used in the shear calculation of experimental beams according to ACI 318-19.[29] The calculated shear capacity values are compared with the experimental results, and these values are offered in Table 6.

$$V_c = 0.66\lambda\sqrt[3]{\rho}\sqrt{f_c}\,b_w d \le V_{c,max} = 0.42\lambda\sqrt{f'_c}\,b_w d A_{sw} \ge 0.35\frac{b_w}{f_{ywk}}s \quad (7)$$

$$V_s = \frac{A_{sw}f_{ywk}}{s}d \le V_{s,max} = 0.66\sqrt{f_c}\,b_w d \quad (8)$$

$$V_n = V_c + V_s \quad (9)$$

where λ is assumed to be 1.0 for normal weight concrete.

There is a difference of maximum 52 and 21%, respectively, between the shear capacities of the reference beams calculated

https://doi.org/10.1021/acsomega.4c05655
ACS Omega 2024, 9, 41662−41675

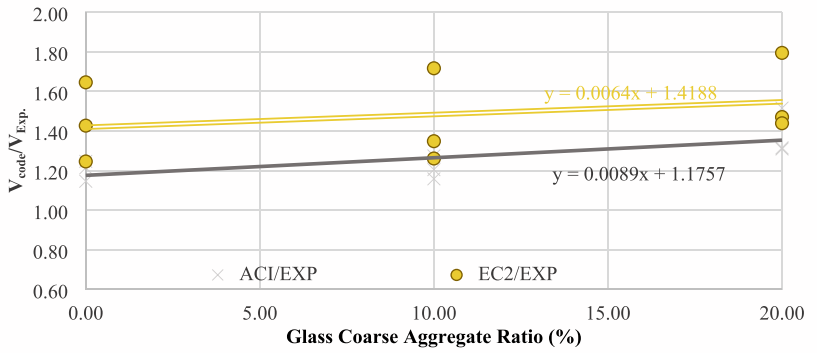

Figure 12. The change in the ratio of specification results to experimental results according to the rate of change of the coarse glass aggregate.

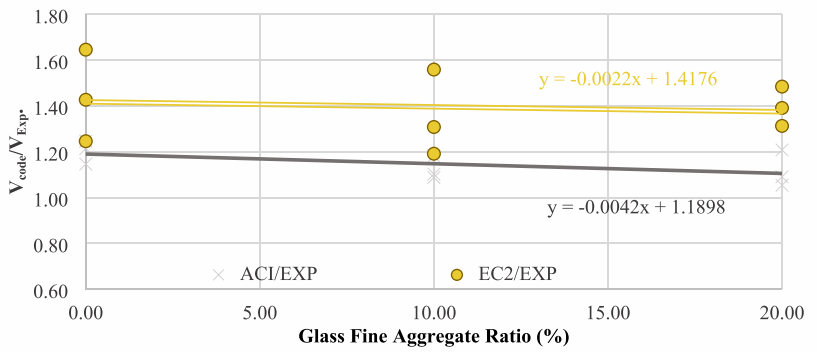

Figure 13. The change in the ratio of specification results to experimental results according to the rate of change of the fine glass aggregate.

by the ACI standard[29] and the results obtained from the experiments. This difference is maximum 79 and 56% in EC2,[28] respectively. As can be noted, the shear capacities calculated by the two standards are higher than those in the experimental results. This situation was caused by the large spacing of the stirrups placed on the beams to prevent shear failure. This is because the stirrup spacing in the beams is much larger (160, 200, and 270 mm) than the maximum stirrup spacing ($d/2$ = 65 mm). However, the results obtained from ACI[29] are much closer to the experimental results than those of EC2.[28] The main reason for this difference is based on the calculation method. As mentioned before, ACI[29] does not consider the effect of the angle (θ) made by the compression bars with the beam axis in its calculation of the shear capacity of the stirrup, according to the classical truss analogy. However, EC2[28] considers this angle in calculations between 21.8° (cot21.8 = 2.5) and 45° (cot45 = 1). Because this angle was calculated as 21.8° in the test beams, the contribution of the stirrups is 2.5 times higher in the calculations. Although EC2[28] limits this contribution with eq 6 to prevent compression crushing of the concrete, the results found with EC2[28] are considerably higher than the experimental results.

Figure 12 illustrates the change in the percentage of specification results to experimental results according to the replacement rate of the glass coarse aggregate. As can be realized from the figure, the proportion of the beam shear capacity calculated with the specification formulas to the experimental results (V_{code}/V_{Exp}) increases as the CA replacement rate increases. In ACI 318-19,[29] the initial error rate is 17.6%, and for every 10% change, this rate increases by an average of 8.9%. On the other hand, in EC2,[28] this error rate is initially 41.9%, and for every 10% increase, this rate increases by an average of 6.4%. There are two possible reasons for this situation. First, as mentioned before, due to the large stirrup spacing, the probability of the crack to coincide with the stirrup decreases; thus, the prediction performance also decreases. The second reason is that the decrease in the shear strength of coarse glass aggregates is greater than the decrease in their compressive and tensile strengths (Table 1). As the replacement of coarse glass aggregate in the concrete mixture increases, the shear strength of the beam decreases much more than expected due to the large volume occupied by the coarse glass aggregate in the combination. From this point of view, it is realized that the difference between the values obtained by the specification formulas and the experimental results increases as the replacement rate increases.

For beams with fine glass aggregate, the change in the ratio of specification results to experimental results was plotted against the substitution rate of the glass fine aggregate. This change is presented in Figure 13. As can be realized from the figure, the ratio of the beam shear capacity calculated with the specification formulas to the experimental results decreases as the fine aggregate substitution rate increases. In ACI 318-19,[29] the initial error rate is 19.0%, and for every 10% change, this rate decreases by an average of 4.2%. However, in EC2,[28] this error rate is initially 41.8%, and for every 10% increase, this rate decreases by an average of 2.2%. Although the initial error rates were due to the stirrup spacing, the gradual decrease in the error rates is due to the fine glass aggregate improving the mechanical properties of the concrete. As a matter of fact, as can be seen in Table 1, as the ratio of fine glass aggregate in the concrete mixture increases, the mechanical strengths of the concrete also increase. This led to an increase in the shear strength of the concrete and reduced the initial failure rate. For this reason, the difference between the values obtained by the specification formulas and the experimental results (V_{code}/

https://doi.org/10.1021/acsomega.4c05655
ACS Omega 2024, 9, 41662−41675

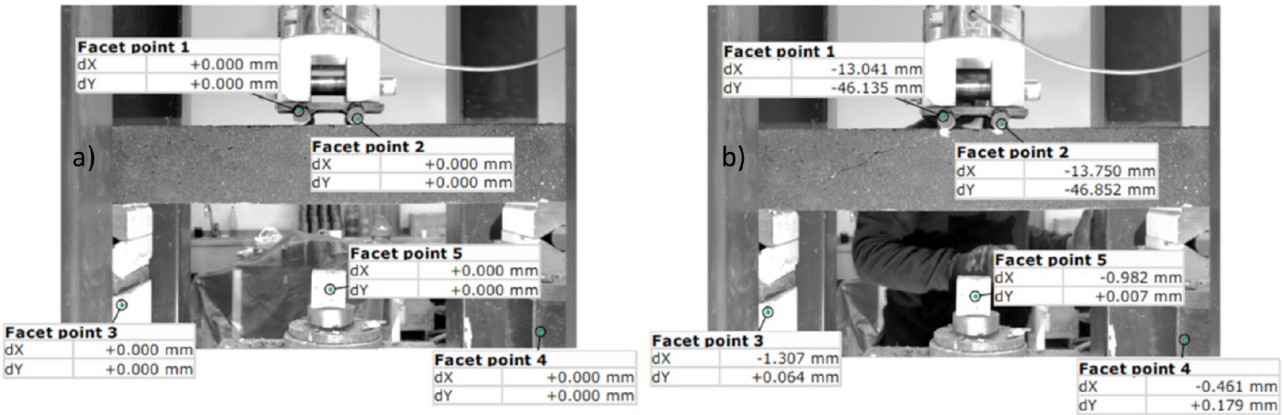

Figure 14. Displacement measurements via digital image correlation (DIC): (a) initial stage and (b) under loading stage.

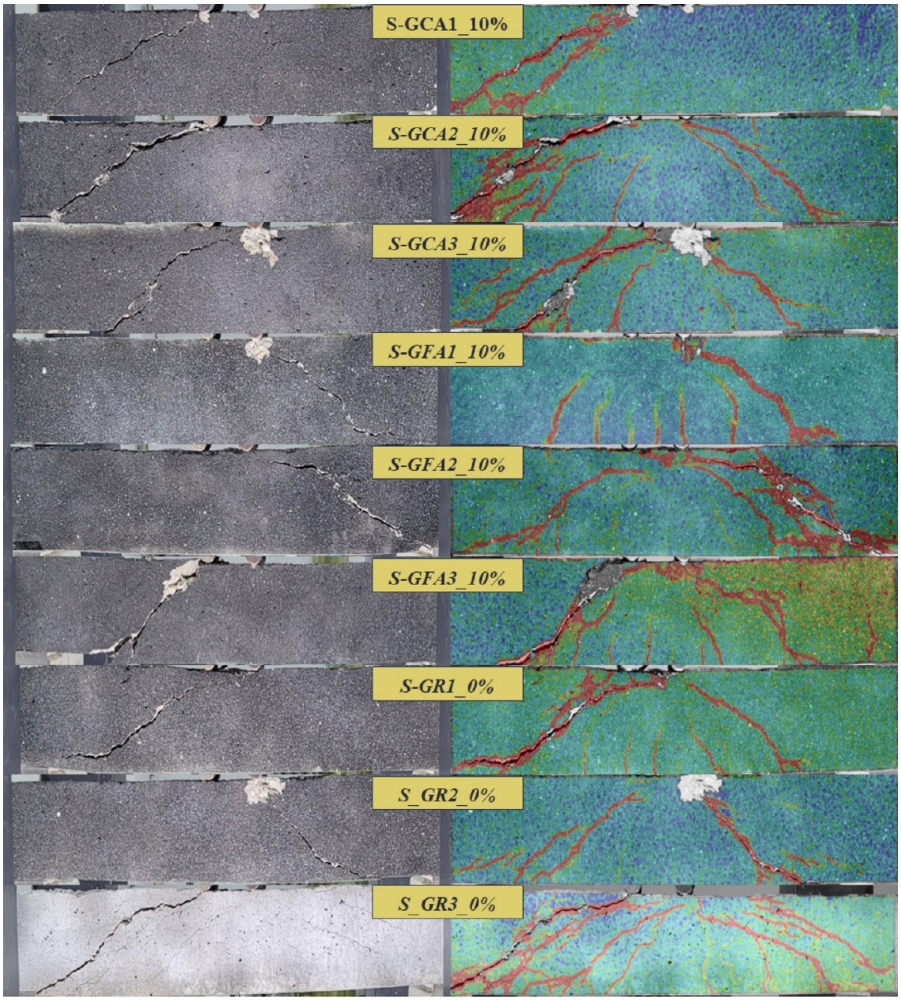

Figure 15. Valuation of the experimental crack reflection and image processing for samples.

V_{Exp}) decreased due to the increase in the substitution rate of the fine glass aggregate.

5. IMAGE PROCESSING TECHNIQUE

Variations in the static and dynamic characteristics of damaged structures generally result in a reduction in the structures' rigidity. In this part of the investigation, image processing method was used to define the microcracks, macro sizes, and large-scale measurements of R-C-B. The purpose of this research is to compare the displacement values measured from the test results of R-C-B with the displacement values measured using the Image Processing Technique. In this manner, it is possible to identify the position and severity of the damage via monitoring of these changes, which also makes it easier to perform prompt repairs and retrofits before the damage continues to deteriorate.

As can be recognized in detail in Figure 3, a camera (Nikon D5300), light source (80w Led), and a computer were used to

https://doi.org/10.1021/acsomega.4c05655
ACS Omega 2024, 9, 41662−41675

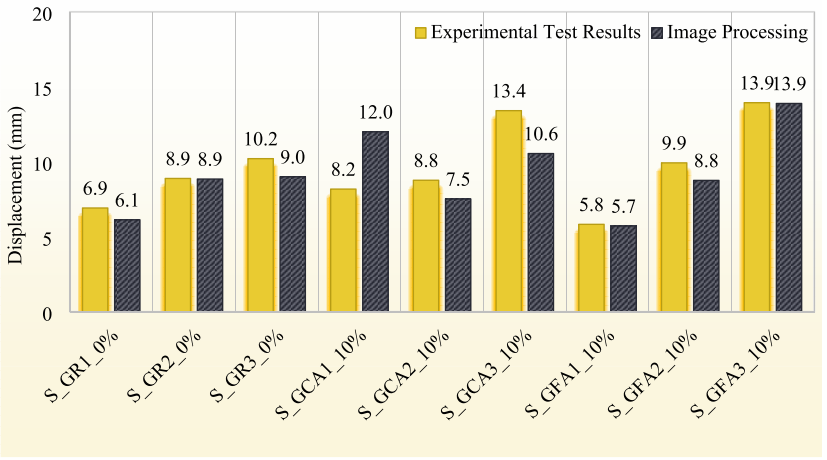

Figure 16. Valuation of the disp. values measured from experimental investigations and image processing.

make a record of the appearance during the experimental investigations. In addition to the loading phase, R-C-B was photographed using a 24.2 megapixel digital camera (Nikon D5300) throughout the experiments. The image capture speed of the digital camera is set to take an image every 4 s. To achieve the image processing, R-C-Bs were painted white color for easy recognition of cracks throughout imaging. The grid shifts obtained from the digital images were converted to the real shift of the R-C-Bs as noticed in Figure 14. From this graph, it can be understood that the lower part of R-C-B has maximum negative values. This situation cares to separate of the real R-C-B example as it is under loads as presented in Figure 14. The observed cracks were illustrated in Figure 15. The failure modes were consistent with the observed cracks in digital imaging. Figure 15 also shows that all strains are reliably evident when the loading is applied, but the crack is not predictable in the R-C-B specimen until beam failure. When the strain pattern is examined, small strains are seen in the *y* direction at the R-C-B base as the loading is gradually increased. This situation continues until the beams failure. However, the strains along the crack change abruptly when the beams fracture. As seen in Figure 16, there is a close agreement between the values obtained from the experimental tests and image processing.

6. CONCLUSIONS

This study investigated the effect of varying amounts of the WG ratio and different stirrup spacings on the shear behavior of R-C-Bs. Furthermore, outcomes measured from test results were compared with the image processing method. The findings of the study are summarized as follows:

The test results further revealed that WGA can be effectively used as a 20% partial replacement for FA. Adding FA to the mixture enhances the shear load-carrying capacity of R-C-Bs. However, increasing the WGA ratio beyond 10% when using CA, along with increasing the stirrup spacing, can significantly reduce the capacity of R-C-Bs.

It was observed that the beam shear capacities calculated with the formulas of the regulations (ACI 318-19 and EC2) for beams with insufficient stirrups were much higher than the experimental results. Because of excessive stirrup spacing, the fracture may not coincide with the stirrups, preventing them from working at full capability. Therefore, the accuracy of the prediction formula is reduced. The estimated shear strengths according to the ACI and EC2 of R-C-Bs with coarse glass aggregate may be up to 52 and 79% higher than experimental values, whereas those with fine glass aggregate can be up to 21 and 56% higher.

In this investigation, the results obtained from the experimental tests were compared with the image processing technique. In the light of the results obtained, it was noticed that the results of the image processing technique are very close to the experimental results. Although the strains obtained through the image processing technique are reliable, the exact location of the crack could not be precisely predicted due to the sudden onset of the shear crack at the moment of beam failure. Therefore, studies in this area should continue, and new technologies should be developed.

The optimal percentage consumptions identified in this study are expected to inform future research. The use of concrete containing WGA in structural members as columns, beams, slabs, etc., can be considered to evaluate structural weight, stiffness, construction time, and seismic productivity.

AUTHOR INFORMATION

Corresponding Authors

Alexey N. Beskopylny − *Department of Transport Systems, Faculty of Roads and Transport Systems, Don State Technical University, Rostov-on-Don 344003, Russia;* orcid.org/0000-0002-6173-9365; Email: besk-an@yandex.ru

Osman Ahmed Umiye − *Department of Civil Engineering, Faculty of Engineering Technolgoy, Zamzam University of Science and Technology, Mogadishu, Somalia; Department of Civil Engineering, Faculty of Engineering, Necmettin Erbakan University, Konya 42000, Turkey;* orcid.org/0009-0005-2755-4366; Email: osmanomiye@zust.edu.so

Yasin Onuralp Özkılıç − *Department of Civil Engineering, Faculty of Engineering, Necmettin Erbakan University, Konya 42000, Turkey; Department of Technical Sciences, Western Caspian University, Baku 1001, Azerbaijan;* Email: yozkilic@erbakan.edu.tr

https://doi.org/10.1021/acsomega.4c05655
ACS Omega 2024, 9, 41662−41675

Authors

Özer Zeybek − *Department of Civil Engineering, Faculty of Engineering, Mugla Sitki Kocman University, Mugla 48000, Turkey*

Boğaçhan Başaran − *Department of Construction, Vocational School of Technical Sciences, Amasya University, Amasya 05100, Turkey*

Ceyhun Aksoylu − *Department of Civil Engineering, Faculty of Engineering and Natural Sciences, Konya Technical University, Konya 42075, Turkey*

Memduh Karalar − *Department of Civil Engineering, Faculty of Engineering, Zonguldak Bulent Ecevit University, Zonguldak 67100, Turkey*

Essam Althaqafi − *Civil Engineering Department, College of Engineering, King Khalid University, Abha 61421, Saudi Arabia*

Sergey A. Stel'makh − *Department of Unique Buildings and Constructions Engineering, Don State Technical University, Rostov-on-Don 344003, Russia*

Evgenii M. Shcherban' − *Department of Engineering Geometry and Computer Graphics, Don State Technical University, Rostov-on-Don 344003, Russia*

Complete contact information is available at: https://pubs.acs.org/10.1021/acsomega.4c05655

Notes

The authors declare no competing financial interest.

■ ACKNOWLEDGMENTS

The authors are thankful for the financial support provided for this research by the Deanship of Scientific Research at King Khalid University, Abha, Saudi Arabia, through Large Groups RGP2/447/45.

■ REFERENCES

(1) Ali, A.; Mahmoud, A. A.; Al Ramadan, M.; Elkatatny, S. The Effect of Olive Waste on the Rheological Properties, Thickening Time, Permeability, and Strength of Oil Well Cement. *ACS omega.* **2023**, *8*, 30139−44.

(2) Sivakrishna, A.; Adesina, A.; Awoyera, P. O.; Rajesh Kumar, K. Green concrete: A review of recent developments. *Mater. Today: Proc.* **2020**, *27*, 54−58.

(3) Miah, M. J.; Huaping, R.; Paul, S. C.; Babafemi, A. J.; Sharma, R.; Jang, J. G. Performance of eco-friendly concrete made from recycled waste tire fine aggregate as a replacement for river sand. *Structures.* **2023**, *58*, No. 105463.

(4) Liu, S.; Zheng, W.; Wu, F. Preparation of ultra-high performance concrete containing waste foundry sand and its application in structures. *Structures.* **2023**, *58*, No. 105472.

(5) Noronha Marques, E.; Bergmann, C. P.; Masuero, A. B. Analysis of the technical feasibility of sustainable concrete production using waste foundry sand as a fine aggregate. *ACS omega.* **2023**, *8*, 46406−13.

(6) Abdelsattar, D. E.; El-Demerdash, S. H.; Zaki, E. G.; Dhmees, A. S.; Azab, M. A.; Elsaeed, S. M.; et al. Effect of Polymer Waste Mix Filler on Polymer Concrete Composites. *ACS omega.* **2023**, *8*, 39730−8.

(7) Gerges, N. N.; Issa, C. A.; Sleiman, E.; Aintrazi, S.; Saadeddine, J.; Abboud, R.; et al. Eco-Friendly Optimum Structural Concrete Mix Design. *Sustainability* **2022**, *14*, 8660.

(8) Özkılıç, Y. O.; Çelik, Aİ; Tunç, U.; Karalar, M.; Deifalla, A.; Alomayri, T.; et al. The use of crushed recycled glass for alkali activated fly ash based geopolymer concrete and prediction of its capacity. *Journal of Materials Research and Technology.* **2023**, *24*, 8267−81.

(9) Çelik, Aİ; Tunç, U.; Bahrami, A.; Karalar, M.; Othuman Mydin, M. A.; Alomayri, T.; et al. Use of waste glass powder toward more sustainable geopolymer concrete. *Journal of Materials Research and Technology.* **2023**, *24*, 8533−46.

(10) Surendran, H.; Akhas, P. K. Properties of high-performance concrete incorporating toughened glass waste coarse aggregate: An experimental study. *Structures.* **2024**, *60*, No. 105897.

(11) Lam, C. S.; Poon, C. S.; Chan, D. Enhancing the performance of pre-cast concrete blocks by incorporating waste glass − ASR consideration. *Cement and Concrete Composites.* **2007**, *29*, 616−25.

(12) Olofinnade, O. M.; Ndambuki, J. M.; Ede, A. N.; Olukanni, D. O. Effect of substitution of crushed waste glass as partial replacement for natural fine and coarse aggregate in concrete. *Trans. Tech. Publ.* **2016**, 58−62.

(13) Tamanna, N.; Tuladhar, R.; Sivakugan, N. Performance of recycled waste glass sand as partial replacement of sand in concrete. *Construction and Building Materials.* **2020**, *239*, No. 117804.

(14) Rahim, N. L.; Che Amat, R.; Ibrahim, N. M.; Salehuddin, S.; Mohammed, S. A.; Abdul, Rahim M Utilization of recycled glass waste as partial replacement of fine aggregate in concrete production. *Trans Tech Publ.* **2014**, 16−20.

(15) Arivalagan, S.; Sethuraman, V. S. Experimental study on the mechanical properties of concrete by partial replacement of glass powder as fine aggregate: An environmental friendly approach. *Materials Today: Proceedings.* **2021**, *45*, 6035−41.

(16) Çelik, Aİ; Özkılıç, Y. O.; Zeybek, Ö; Karalar, M.; Qaidi, S.; Ahmad, J.; et al. Mechanical behavior of crushed waste glass as replacement of aggregates. *Materials.* **2022**, *15*, 8093.

(17) Hama, S. M.; Mahmoud, A. S.; Yassen, M. M. Flexural behavior of reinforced concrete beam incorporating waste glass powder. *Structures.* **2019**, *20*, 510−8.

(18) Haido, J. H.; Zainalabdeen, M. A.; Tayeh, B. A. Experimental and numerical studies on flexural behavior of high strength concrete beams containing waste glass. *Adv. Concrete Construct.* **2021**, *11*, 239.

(19) Sharba, A.Possibility of using waste glass powder and ceramic tile as an aggregate on the flexural behavior and strength properties. *Proceedings of the 1st International Multi-Disciplinary Conference Theme: Sustainable Development and Smart Planning, IMDC-SDSP 2020, Cyperspace*; EAI 2020, DOI: ...

(20) Amin, M. N.; Alkadhim, H. A.; Ahmad, W.; Khan, K.; Alabduljabbar, H.; Mohamed, A. Experimental and machine learning approaches to investigate the effect of waste glass powder on the flexural strength of cement mortar. *PloS one.* **2023**, *18*, No. e0280761.

(21) Kumar, M. H.; Mohanta, N. R.; Samantaray, S.; Kumar, N. M. Combined effect of waste glass powder and recycled steel fibers on mechanical behavior of concrete. *SN Appl. Sci.* **2021**, *3* (2021), 350−368.

(22) Mustafa, T. S.; El. Beshlawy, S. A.; Nassem, A. R. Experimental study on the behavior of RC beams containing recycled glass. *Construction and Building Materials.* **2022**, *344*, No. 128250.

(23) Hamada, H. M.; Abed, F.; Binti Katman, H. Y.; Humada, A. M.; Al Jawahery, M. S.; Majdi, A.; Yousif, S. T.; Thomas, B. S.; et al. Effect of silica fume on the properties of sustainable cement concrete. *Journal of Materials Research and Technology.* **2023**, *24*, 8887−908.

(24) Hamada, H.; Shi, J.; Yousif, S. T.; Al Jawahery, M.; Tayeh, B.; Jokhio, G. Use of nano-silica in cement-based materials−a comprehensive review. *Journal of Sustainable Cement-Based Materials.* **2023**, *12*, 1286−306.

(25) Hamada, H. M.; Shi, J.; Abed, F.; Al Jawahery, M. S.; Majdi, A.; Yousif, S. T. Recycling solid waste to produce eco-friendly ultra-high performance concrete: A review of durability, microstructure and environment characteristics. *Science of The Total Environment.* **2023**, *876*, No. 162804.

(26) Hamada, H. M.; Shi, J.; Abed, F.; Humada, A. M.; Majdi, A. Recycling solid waste to produce eco-friendly foamed concrete: A comprehensive review of approaches. *Journal of Environmental Chemical Engineering.* **2023**, *11*, No. 111353.

(27) *European Committee for S. EN 206:2013+ A1:2016 Concrete—Specification, performance, production and conformity*. European Committee for StandardizationBrussels, Belgium, 2016.
(28) En, B. S.. 1−1:2004 Eurocode 2: Design of concrete structures. General rules and rules for buildings.*General rules and rules for buildings* 1992;3.
(29) Aci, C.*ACI 318−19: Building Code Requirements for Structural Concrete and Commentary*. Farmington Hills, MI, USA: American Concrete Institute. 2019.

https://doi.org/10.1021/acsomega.4c05655
ACS Omega 2024, 9, 41662−41675